THE JOURNAL OF PHYSICAL CHEMISTRY B

Article

pubs.acs.org/JPCB

Explicit Solvent Molecular Dynamics Simulations of Aβ Peptide Interacting with Ibuprofen Ligands

Christopher Lockhart, Seongwon Kim, and Dmitri K. Klimov*

School of Systems Biology, George Mason University, Manassas, Virginia 20110, United States

Supporting Information

ABSTRACT: Using all-atom explicit water model and replica exchange molecular dynamics, we study the interactions between Aβ monomer and nonsteroidal anti-inflammatory drug ibuprofen, which is known to reduce the risk of Alzheimer's disease. Ibuprofen binding to Aβ is largely governed by hydrophobic effect, and its binding site in Aβ peptide is entirely composed of hydrophobic amino acids. Electrostatic interactions between negatively charged ibuprofen ligands and positively charged side chains make a relatively small contribution to binding. This outcome is explained by the competition of ligand−peptide electrostatic interactions with intrapeptide salt bridges. Consistent with the experiments, the S-isomer of ibuprofen binds with stronger affinity to Aβ than the R-isomer. Conformational ensemble of Aβ monomer in ibuprofen solution reveals two structured regions, 19−25 (R1) and 29−35 (R2), composed of turn/helix and helix structure, respectively. The clustering technique and free energy analysis suggest that Aβ conformational ensemble is mainly determined by the formation of Asp23-Lys28 salt bridge and the hydrophobic interactions between R1 and R2. Control simulations of Aβ peptide in ligand-free water show that ibuprofen binding changes Aβ structure by promoting the formation of helix and Asp23-Lys28 salt bridge. Implications of our findings for Aβ amyloidogenesis are discussed.

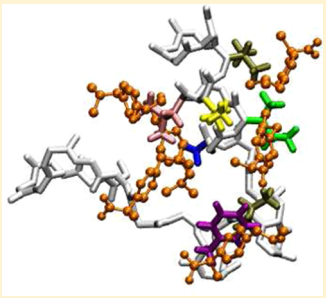

INTRODUCTION

Biomedical and genetic studies have linked the aggregation of Aβ peptides to the onset of Alzheimer's disease (AD).[1,2] Aβ aggregation pathway proceeds through a complex sequence of structural transitions, which starts with the oligomerization of monomeric peptides and eventually leads to the formation of amyloid fibrils.[3] Cellular proteolysis produces multiple Aβ alloforms, among which a 40-residue peptide $A\beta_{1-40}$ is most abundant. Experimental data indicate that Aβ oligomers, even as small as dimers, are the primary cytotoxic species in AD.[4]

Critical role of Aβ peptides in AD pathogenesis has prompted a search for small molecular agents, which can block or at least control Aβ aggregation. Among the potential antiaggregation agents is a nonsteroidal anti-inflammatory drug (NSAID) ibuprofen.[5] Epidemiological studies have shown that prophylactic intake of ibuprofen reduces the risk of AD approximately in half.[6,7] At the same time, the effectiveness of this drug against preexisting AD conditions appears to be very limited.[8] *In vivo* biomedical studies suggest that treatment with ibuprofen reduces the amount of Aβ deposits and alleviates memory deficits in mice models.[9,10] Furthermore, ibuprofen intake correlates with the decrease in the load of Aβ oligomers in mice brain tissues.[10] Several recent *in vitro* studies have investigated the interactions between Aβ and ibuprofen. Binding of ibuprofen to Aβ fibrils has been demonstrated when the ligand:peptide stoichiometric ratio is about or exceeds 1.[11] Experimental *in vitro* studies have also shown that ibuprofen reduces the accumulation of Aβ fibrils by apparent interference with the fibril elongation.[12]

Although experiments have demonstrated the antiaggregation action of ibuprofen, the molecular mechanisms of its binding to Aβ species remain elusive. For example, no information is available on the location of ibuprofen binding sites in Aβ peptides and, more generally, on the physicochemical factors, which control ibuprofen−Aβ interactions. It is also unclear if ibuprofen binding biases the conformational ensemble of Aβ peptides. A useful tool to address these questions is molecular dynamics (MD) simulations, which can map the interactions of Aβ with the ligands at all-atom resolution.[13,14] Utilizing this approach, a number of recent MD studies have probed binding of small molecule ligands to amyloidogenic peptides.[15−19] For example, implicit solvent MD has been applied to study binding of small aromatic ligands to the $A\beta_{12-28}$ fragment. Their binding was shown to induce minor changes in the peptide structural ensemble, and no specific binding locations in the peptide were observed.[17] Explicit solvent MD has been used to explore binding of flavonoids to Aβ fibrils.[15] The results revealed ligand binding to the fibril edges and their penetration into fibril hydrophobic core. In our previous implicit solvent simulations, we have investigated binding of NSAID ligands to Aβ fibrils and oligomers and their antiaggregation potential.[20−24] These studies have shown that NSAID ligands interfere with interpeptide interactions and some also change peptide conformations. However, simplicity of implicit solvent model

Received: June 24, 2012
Revised: October 10, 2012
Published: October 10, 2012

dx.doi.org/10.1021/jp306208n | J. Phys. Chem. B 2012, 116, 12922−12932

may not have captured all the details of ibuprofen binding mechanism.

Recent experiments have shown that Aβ aggregation inhibitors generally induce helix structure in this peptide.[25] Intrigued by this possibility, we reexamine the binding of ibuprofen to Aβ monomers using more accurate all-atom explicit solvent model and replica exchange molecular dynamics (REMD). We show that the main factor controlling ibuprofen binding is the hydrophobic effect, whereas electrostatic or ligand−ligand interactions are less important. Our simulations suggest that the S-isomer of ibuprofen has higher binding affinity than the R-isomer, and we offer a plausible reason for this difference. We further show that conformational ensemble of Aβ peptide in ibuprofen solution is mainly determined by the closure and rupture of Asp23-Lys28 salt bridge and the hydrophobic contacts between Phe19, Val24, and Ile31 side chains. We found that the conformational ensemble of Aβ monomer in ligand-free water is markedly different, suggesting that ibuprofen induces structural changes in Aβ.

MODEL AND SIMULATION METHODS

All-Atom Explicit Solvent Model. Molecular simulations of Aβ monomer and ibuprofen ligands were performed using all-atom explicit solvent CHARMM22 force field with CMAP corrections,[26] which were shown to improve the agreement between experimental protein structures and those generated by MD, especially in the unstructured regions.[26] For ibuprofen we used the parametrization developed by Harvey and co-workers on the basis of quantum mechanical calculations.[27]

Following our previous studies,[20] we have selected Aβ_{10-40} peptide, the N-terminal truncated fragment of the full-length Aβ_{1-40} (Figure 1a). Experiments[28] and simulations[29] have revealed similarities between Aβ_{1-40} and Aβ_{10-40} oligomers in terms of size distributions and structure. In addition, as recently shown, the N-terminal fragment of Aβ_{1-40} monomer does not form extensive long-range interactions or ordered secondary structure.[30] Consequently, we use Aβ_{10-40} as an approximate model for probing ibuprofen binding to Aβ_{1-40} peptide. It must be pointed out that Aβ_{10-40} rarely occurs *in vivo*,[31] and amino-terminal residues truncated from Aβ_{1-40} may contribute to ibuprofen binding (see Discussion for more details).

The simulation system consists of Aβ_{10-40} monomer interacting with 10 ibuprofen ligands (Figure 1b,c) placed in the 59 Å × 59 Å × 59 Å box with 6313 TIP3P water molecules. To neutralize the system charge, 11 sodium ions were added. As a control system, we have considered an Aβ monomer in the ligand-free water box with the dimensions 53.8 Å × 53.8 Å × 53.8 Å. Simulations were performed by applying periodic boundary conditions. Electrostatic interactions were computed using Ewald summation. The van der Waals interactions were smoothly switched off in the interval from 8 to 12 Å. All covalent bonds were constrained by the SHAKE algorithm. The concentration ratio of ibuprofen to Aβ peptide, i.e., the ratio of the numbers of ligands and peptides, is 10:1, which is within the *in vitro* experimental range (from 1:1 to 22:1)[12,32] and is consistent with *in vivo* measurements of Aβ and ibuprofen concentrations in cerebrospinal fluid and plasma.[33,34] Ibuprofen molecule can adopt two isomeric forms, R and S, determined by the sign of the improper angle formed by the atoms C4, C7, C8, and C9 (Figure 1d). In our simulation system eight ibuprofens out of ten are R-isomers and two are S. This particular ratio of isomers was chosen at random. A snapshot of simulation system is shown in Figure 1c. Comparison of Aβ monomer experimental and computational structures is presented in the Supporting Information.

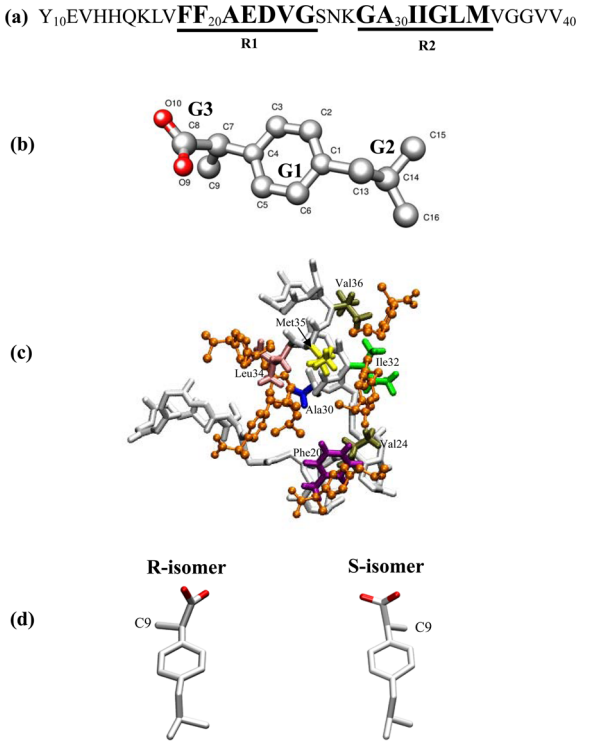

Figure 1. (a) The sequence of amino-terminal truncated Aβ_{10-40} peptide and the locations of the structured R1 and R2 regions (in bold). (b) Three structural moieties compose ibuprofen molecule—hydrophobic phenyl G1 and isobutyl G2 and hydrophilic carboxylate G3 groups. Carbon and oxygen atoms are in gray and red; hydrogen atoms are not shown. (c) Snapshot of Aβ_{10-40} monomer with bound ibuprofen ligands (in orange) at 330 K. The side chains composing the ibuprofen binding site are shown: Phe20 (in purple), Val24 (in dark gray), Ala30 (in blue), Ile32 (in green), Leu34 (in pink), Met35 (in yellow), and Val36 (in dark gray). Aβ backbone is light gray. Unbound ligands and water are not shown for clarity. (d) Ibuprofen exists in two isomeric states, R and S, which differ with respect to the position of carbon C9 (see Model and Simulation Methods for details).

Replica Exchange Protocol. Conformational sampling for Aβ monomer in ibuprofen solution was performed using the replica exchange method[35] coupled with the NAMD MD program.[36] In all, 40 replicas were distributed exponentially in the temperature range from 300 to 440 K. Canonical ensembles in the replicas were generated using underdamped Langevin simulations of "virtual" solvent with the damping coefficient γ = 5 ps^{-1} and the integration step of 1 fs. Exchanges were attempted every 2 ps between all neighboring replicas with the average acceptance rate of 24%. Four REMD trajectories were produced resulting in a cumulative simulation time of 3.2 μs or 80 ns per replica. Because the initial parts of REMD trajectories are not equilibrated and must be excluded from thermodynamic analysis, the cumulative equilibrium simulation time was reduced to $\tau_{sim} \approx 2.9$ μs. The REMD trajectories were started with random distributions of Aβ peptide and ligands. The REMD simulations for the ligand-free system followed the same protocol, except for the cumulative simulation time, which was reduced to 40 ns per replica. The average acceptance rate was 29%. Compared to the system with the ligands, the simulation time for the ligand-free system was shorter because previous studies have shown that the Aβ_{1-40} monomer should

dx.doi.org/10.1021/jp306208n | J. Phys. Chem. B 2012, 116, 12922−12932

be simulated for at least 20 ns per replica to achieve sampling convergence.[37] The analysis of REMD convergence, equilibration, and errors is presented in the Supporting Information.

Computation of Structural Probes. Interactions formed by Aβ peptide and ibuprofen were probed as follows. An intrapeptide contact between amino acid side chains occurs, if the distance between their centers of mass is less than 6.5 Å. This cutoff approximately corresponds to the onset of hydration of side chains as their separation increases. Ibuprofen molecule contains three structural groups (Figure 1b), of which G1 and G2 are hydrophobic and G3 is hydrophilic. A contact with Aβ side chain occurs if the distance between the centers of mass of side chain and one of the ibuprofen groups is less than 6.5 Å. If the contact involves G1 or G2 and hydrophobic side chain, then it is assumed hydrophobic. A contact between two ibuprofen molecules is formed if any of the G1−G3 centers of mass from different molecules are within 6.5 Å distance. Ibuprofen is considered bound if it forms at least one contact with Aβ (Figure 1c). Ibuprofen molecule is self-aggregated if it forms contact with at least one other ligand. Hydrogen bonds (HB) between peptide NH and CO groups and between ibuprofen and peptide backbone were assigned according to Kabsch and Sander.[38]

Secondary structure in Aβ peptide was computed using the STRIDE program[39] and by analyzing the distributions of backbone dihedral angles (ϕ, ψ) as described in our previous studies.[40] Accessible surface area (ASA) of Aβ peptide and ibuprofen was computed using the VMD program by taking into account all atoms including hydrogens and setting the probe radius to 1.4 Å.[41] Hydrophobic accessible surface area (hASA) of amino acid is defined as a sum of ASA values for all apolar atoms in the respective side chain. Relative hASA of amino acid X is obtained by dividing the hASA of amino acid X by its ASA in the reference triplet state Gly-X-Gly.[42] Relative polar accessible surface area (pASA) of amino acid is defined in a similar way considering only polar atoms.

The energetics of ligand binding and side-chain interactions was computed using saved REMD trajectories and namdenergy module in VMD applying smooth switching function from 8 to 12 Å and without using Ewald summation. The van der Waals and electrostatic energies are highly sensitive to the topology and force field parameters such as partial charges. Therefore, ibuprofen binding mechanism reported in our study depends on the accuracy of B3LYP/6-31G* calculations of Harvey and co-workers[27] used for parametrizing this ligand and on the quality of CHARMM force field in general. Thermodynamic averages of structural quantities (denoted as $\langle ... \rangle$) and free energy landscapes were computed using the multiple histogram method.[43] The analysis of Aβ conformational ensemble was performed using clustering technique described in the Supporting Information.

RESULTS

Ibuprofen Binds to Aβ Peptide. Using REMD sampling, we have examined the binding of ibuprofen ligands to Aβ peptide. At 330 K the number of bound ligands $\langle L \rangle$ is 3.8. Because the total number of ligands in the system is 10, the probability of binding (i.e., the binding affinity) for ibuprofen molecule is P_b = 0.38. To investigate binding affinities of ibuprofen structural groups G1−G3 (Figure 1b), we computed their individual binding probabilities, P_b(G1), P_b(G2), and P_b(G3). The isobutyl group G2 has the strongest binding affinity (P_b(G2) = 0.34) followed by the aromatic G1 (P_b(G1) = 0.31) and polar G3 (P_b(G3) = 0.25). (Note that the errors in P_b are <0.01.) The number of ligands bound via hydrophobic interactions is $\langle L_h \rangle$ = 3.2 or 83% of the total number bound. The binding free energy landscape was probed by the free energy of a ligand $F(r_b)$ as a function of the distance to Aβ surface r_b. Figure 2a shows that $F(r_b)$ has two minima

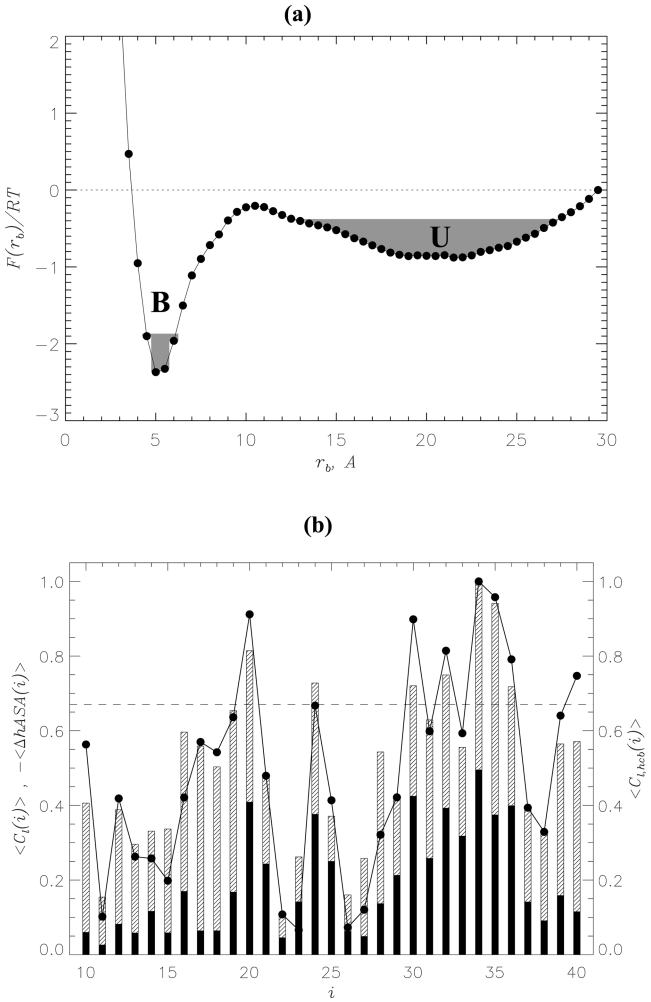

Figure 2. (a) Free energy of ibuprofen ligand, $F(r_b)$, as a function of the distance to Aβ surface, r_b, at 330 K. Two minima in $F(r_b)$ represent the bound (B) and unbound (U) ibuprofen states. The free energies of B and U, F_B and F_U, are computed by integrating the shadowed states with $F < F_{min} + 0.5RT$, where F_{min} is a minimum in B or U state. (b) The numbers of contacts formed by Aβ amino acid side chains i with the ligands, $\langle C_l(i) \rangle$, at 330 K normalized by the maximum value (shaded bars). Black bars represent the numbers of Aβ−ligand contacts, $\langle C_{l,hcb}(i) \rangle$, involved in the formation of helix-stabilizing cross-bridges normalized by the maximum $\langle C_l(i) \rangle$. The changes in relative hydrophobic ASA $\langle \Delta hASA(i) \rangle$ of amino acids i are shown by black circles. Dashed line marks the threshold value ($2/3 \max_i(\langle C_l(i) \rangle)$) used to define the ibuprofen binding site. This panel reveals a strong correlation between the number of ligand−peptide contacts and the reduction in hydrophobic ASA.

associated with the bound (B, $F_B = -3.5RT$ at $r_b \approx 5$ Å) and unbound (U, $F_U = -4.1RT$ at $r_b \sim 20$ Å) states. Consistent with the value of binding probability P_b, the free energy profile in Figure 2a suggests that a slight majority of ibuprofen ligands remain unbound at 330 K. At 300 K the binding probability P_b increases to 0.44.

dx.doi.org/10.1021/jp306208n | J. Phys. Chem. B 2012, 116, 12922−12932

Interactions of ligands with individual amino acids can be analyzed using the number of contacts formed by Aβ amino acid side chain i with the ligands, $\langle C_l(i)\rangle$ (Figure 2b). On an average, at 330 K hydrophobic amino acids form 0.54 ± 0.01 contacts with the ligands, whereas positively charged amino acids make 0.46 ± 0.02 contacts. For comparison, neutral polar and negatively charged amino acids form 0.28 ± 0.01 and 0.14 ± 0.01 contacts. Using the normalized plot of $\langle C_l(i)\rangle$ in Figure 2b, we define the binding site to include the amino acids i, for which $\langle C_l(i)\rangle > 2/3\max_i(\langle C_l(i)\rangle)$. Then, the ibuprofen binding site consists of seven amino acids, namely, Phe20 (0.81), Val24 (0.73), Ala30 (0.72), Ile32 (0.75), Leu34 (1.0), Met35 (0.94), and Val36 (0.72) (the numbers in parentheses are the normalized $\langle C_l(i)\rangle$). Importantly, the binding site is exclusively composed of hydrophobic amino acids. A representative structure of Aβ peptide with bound ligands is displayed in Figure 1c.

To test the importance of ligand−peptide hydrophobic interactions, we analyzed the change in relative hydrophobic accessible surface area $\langle \Delta h\mathrm{ASA}(i)\rangle$ of amino acids i (see Model and Simulation Methods). Specifically, we define $\langle \Delta h\mathrm{ASA}(i)\rangle = \langle \Delta h\mathrm{ASA_b}(i)\rangle - \langle \Delta h\mathrm{ASA_u}(i)\rangle$, where $\langle \Delta h\mathrm{ASA_b}(i)\rangle$ and $\langle \Delta h\mathrm{ASA_u}(i)\rangle$ are the relative hydrophobic ASAs of amino acid i with ibuprofen molecules bound or removed, respectively. Figure 2b demonstrates that $\langle \Delta h\mathrm{ASA}(i)\rangle$ strongly correlates with $\langle C_l(i)\rangle$, which measures the number of ligand−peptide interactions (correlation factor is 0.94). Furthermore, on an average, binding of ibuprofen decreases the absolute $\langle h\mathrm{ASA}\rangle$ for hydrophobic, positively charged, neutral polar, and negatively charged amino acids by 15.3, 10.2, 5.5, and 2.0 Å^2, respectively. Therefore, taken together our results imply that binding of ibuprofen to Aβ peptide is mainly governed by hydrophobic effect.

The binding energetics was probed by computing nonbonded (van der Waals and electrostatic) interactions between Aβ and ligands (see Model and Simulation Methods for details). The average energy of interaction between a bound ibuprofen and Aβ peptide, $\langle E_{lp}\rangle$, is −23.6 kcal/mol, whereas the average energy of ligand−ligand interactions, $\langle E_{ll}\rangle$, is 2.1 kcal/mol. The contributions of van der Waals and electrostatic interactions to $\langle E_{ll}\rangle$ are −2.0 and 4.1, respectively. Therefore, due to negative charges on G3 groups, the interactions between bound ibuprofen ligands are repulsive. In this context, it is of interest to analyze the self-aggregation of bound ibuprofen ligands. (To this end, we considered only ligands already bound to the peptide as defined in Model and Simulation Methods. A ligand is assumed self-aggregated if it forms at least one contact with other ligand.) By computing the probability distribution for the sizes of clusters formed by the ligands bound to Aβ,[22] we found that 57% of those ligands self-aggregate at 330 K; i.e., they participate in the clusters of two or more ligands. This implies that attractive ligand−peptide interactions compensate repulsive ligand−ligand interactions.

Ibuprofen molecule can adopt two isomeric states, R and S, which are known from the experiments to have different binding affinities to Aβ (Figure 1d).[11] To compare their *in silico* affinities, Figure S6 shows the probabilities of binding, $P_b^R(i)$ and $P_b^S(i)$, of the R- and S-isomers to the side chains of amino acids i. This plot reveals that the binding affinity of S-isomer exceeds that of R for almost all Aβ amino acids. Indeed, the probability of binding of the S molecule to Aβ is $P_b^S = 0.43 \pm 0.04$ compared to $P_b^R = 0.37 \pm 0.01$ for the R-isomer. (Note that these probabilities refer to single R or S ligands.)

Aβ Conformational Ensemble. Our next step is to investigate the conformational ensemble of Aβ peptide coincubated with ibuprofen ligands. At 330 K the overall fractions of helical $\langle h\rangle$, random coil $\langle rc\rangle$, and turn $\langle t\rangle$ structures in Aβ computed using STRIDE are 0.33, 0.32, and 0.35, respectively. The contribution from other types of secondary structure is less than 0.01. Figure 3a shows the fractions of helical $\langle h(i)\rangle$, random coil $\langle rc(i)\rangle$, and turn $\langle t(i)\rangle$ structures formed by individual residues i. There are two regions, in which helical or turn structure dominate the conformational ensemble: residues 19−25 (R1) and 29−35 (R2). In R1, the average fractions of turn and helix structure formed by residue, $\langle t(\mathrm{R1})\rangle$ and $\langle h(\mathrm{R1})\rangle$, are 0.54 and 0.30. In R2, $\langle h(\mathrm{R2})\rangle$ reaches 0.74. In both regions, the fractions of random coil $\langle rc\rangle$ are less

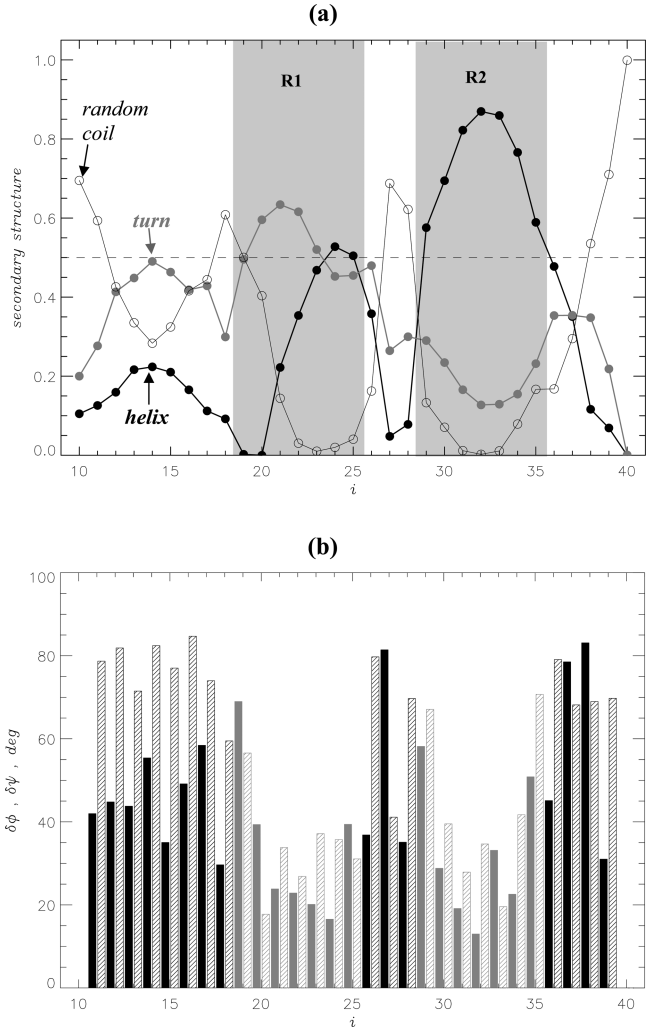

Figure 3. (a) Distribution of secondary structure in Aβ monomer computed by STRIDE: fractions of helical $\langle h(i)\rangle$ (black filled circles), random coil $\langle rc(i)\rangle$ (open circles), and turn $\langle t(i)\rangle$ (gray filled circles) structure formed by residues i. The plot reveals two structured regions, in which either helical or turn structure dominates (>0.5): 19−25 (R1) and 29−35 (R2). (b) Standard deviations, $\delta\phi(i)$ (filled bars) and $\delta\psi(i)$ (shaded bars), of the backbone dihedral angles ϕ and ψ for residue i in Aβ monomer. The structured regions R1 and R2 are shown in gray; the rest of Aβ sequence is in black. This plot demonstrates that peptide structural fluctuations are suppressed in R1 and R2. Both panels are computed at 330 K for Aβ peptide coincubated with ibuprofen.

dx.doi.org/10.1021/jp306208n | J. Phys. Chem. B 2012, 116, 12922−12932

than 0.16, whereas elsewhere in Aβ peptide $\langle rc \rangle \approx 0.5$. Insight into the distribution of structural fluctuations in Aβ peptide is provided by the standard deviations $\delta\phi(i)$ and $\delta\psi(i)$ of the backbone dihedral angles ϕ and ψ for residues i. According to Figure 3b, two structured regions R1 and R2 identified in Figure 3a match the sequence intervals with suppressed fluctuations. For instance, the average standard deviation in ϕ and ψ angles in R1 and R2 is 36°, whereas in unstructured Aβ regions it is almost twice larger (61°).

Folding of Aβ peptide can be probed by the intrapeptide contact map $\langle C(i,j) \rangle$, which reports the equilibrium probabilities of forming side chain contacts between the residues i and j. Figure 4a demonstrates that Aβ peptide coincubated with ibuprofen forms a mixture of local ($|j - i| < 5$) and long-range ($|j - i| \geq 5$) contacts. Specifically, at 330 K the total number of intrapeptide contacts is $\langle C \rangle = 28.1$, of which $\langle C_{LR} \rangle = 11.3$ or 40% are the long-range contacts. Few of such contacts are quite stable ($\langle C(i,j) \rangle > 0.35$), including Asp23-Lys28 (0.53), Phe19-Ile31 (0.47), Asp23-Ile31 (0.45), and Val24-Ile31 (0.43)

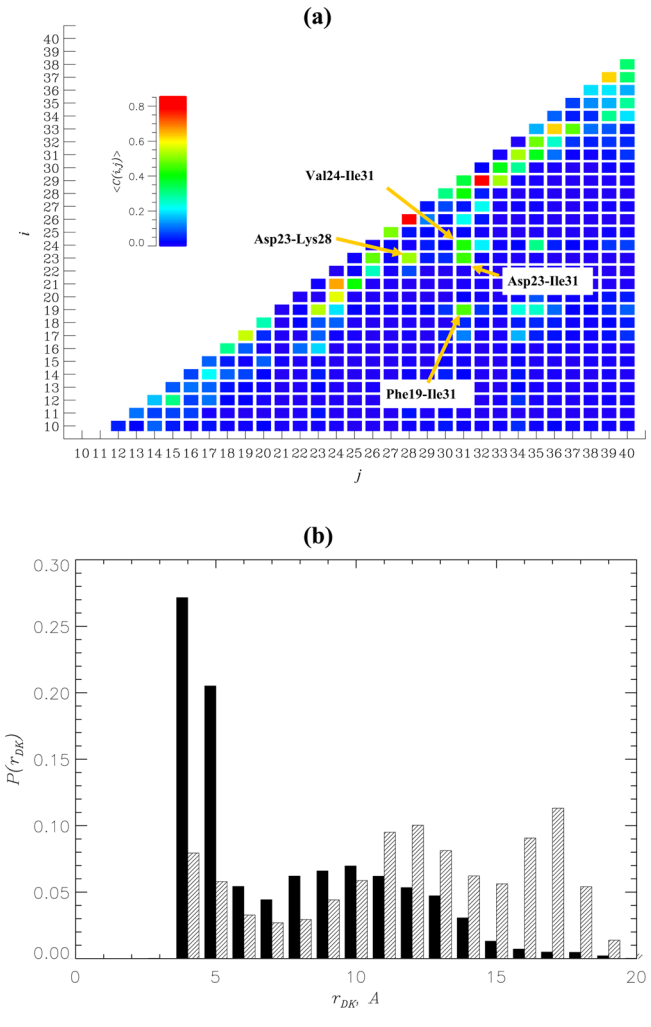

Figure 4. (a) Intrapeptide contact map $\langle C(i,j) \rangle$ shows the equilibrium probabilities of forming side chain contacts between the residues i and j in ibuprofen solution. Four most stable long-range contacts ($|i - j| \geq 5$) are indicated. The values of $\langle C(i,j) \rangle$ are color coded according to the scale. (b) Probability distributions $P(r_{DK})$ of distances r_{DK} between the side chains of Asp23 and Lys28 in ibuprofen solution (solid black bars) and in ligand-free water (shaded bars). Both plots are computed at 330 K.

(Figure 4a). These interactions suggest that (i) the most stable contacts are formed between the residues from the R1, R2, or adjacent regions and (ii) the salt bridge Asp23-Lys28, also found in the fibril structures,[44] is marginally stable and represents the strongest pairwise interaction between residues. The last point is illustrated in Figure 4b, which shows a bimodal distribution of distances r_{DK} between Asp23 and Lys28.

To map the ensemble of Aβ conformations, we applied the clustering algorithm (see Supporting Information). Aβ structures can be grouped in four clusters, which taken together encompass 97% of structures at 330 K (Figure 5). (In what follows, a contact between residues i and j is assumed stable in a given cluster, if $C(i,j) > 0.5$.) The most populated cluster CL1 (probability of occurrence is $P_{CL} = 0.33$) lacks stable long-range contacts, and the Asp23-Lys28 salt bridge is disrupted ($C(23,28) = 0.40$). The second most populated cluster CL2 ($P_{CL} = 0.25$) contains four stable long-range contacts: Phe19-Ile31 ($C(19,31) = 0.78$), Asp23-Lys28 (0.82), Asp23-Ile31 (0.63), and Val24-Ile31 (0.75). In CL2 the Asp23-Lys28 salt bridge is formed, and most of the stable interactions (three out of four) are "anchored" by the hydrophobic Ile31 from the R2 region. The third cluster CL3 ($P_{CL} = 0.20$) is characterized by the most extensive network of stable long-range interactions, which includes Phe19-Ile31 (0.73), Asp23-Lys28 (0.87), Asp23-Ile31 (0.88), Val24-Ile31 (0.72), Val24-Ile32 (0.55), and Val24-Met35 (0.91). As in CL2 the Asp23-Lys28 salt bridge is formed, and two residues, Val24 from R1 and Ile31 from R2, emerge as interaction "hubs". Finally, four stable long-range contacts are observed in the fourth cluster CL4 ($P_{CL} = 0.19$), which are Phe19-Ile31 (0.55), Phe19-Met35 (0.62), Asp23-Ile31 (0.61), and Ser26-Ile31 (0.88). In CL4, the Asp23-Lys28 salt bridge is disrupted, and as in CL2 hydrophobic residue Ile31 forms most of stable long-range contacts. The distribution of interactions in CL1−CL4 demonstrates that two hydrophobic amino acids, Ile31 and Val24, act as interaction "hubs", and all residues involved in stable long-range interactions are from or proximal to the structured regions R1 and R2. Thus, cluster analysis suggests that Aβ structures primarily differ with respect to the number of R1−R2 contacts and the formation of the Asp23-Lys28 salt bridge. Other structural characteristics of CL1−CL4 are similar (see Supporting Information).

To investigate the free energy landscape underpinning the cluster distribution in Figure 5, we projected the free energy of Aβ peptide $F(r_{DK},C_{CL})$ as a function of the distance between the side chains of Asp23 and Lys28, r_{DK}, and the number of intrapeptide contacts, C_{CL}, formed between the amino acids involved in stable interactions in CL1-CL4 (Phe19, Asp23, Val24, Ser26, Ile31, Ile32, Met35). The free energy landscape in Figure 6 reveals two basins, in which Asp23-Lys28 salt bridge is either formed (ON, $r_{DK} \lesssim 5$ Å) or disrupted (OFF, $r_{DK} \sim 10$ Å). The clusters CL2 and CL3 can be mapped to the narrow ON basin, whereas CL1 and CL4 are associated with the wide shallow OFF minimum, which has two sub-basins. To compute the free energy of the ON state, F_{ON}, we integrate the free energies in the ON basin $F(r_{DK},C_{CL}) < F_{min} + 0.4RT$, where F_{min} is the minimum in ON. A similar approach was used to obtain the free energy of the OFF state, F_{OFF}. Then, the free energy gap between the ON and OFF is $\Delta F = F_{ON} - F_{OFF} = 0.1RT$; i.e., the thermal weights of both states are about the same at 330 K. This conclusion is in agreement with the marginal stability of Asp23-Lys28 salt bridge ($\langle C(23,28) \rangle = 0.53$) (Figure 4). The free energy barrier for disrupting the

dx.doi.org/10.1021/jp306208n | J. Phys. Chem. B 2012, 116, 12922−12932

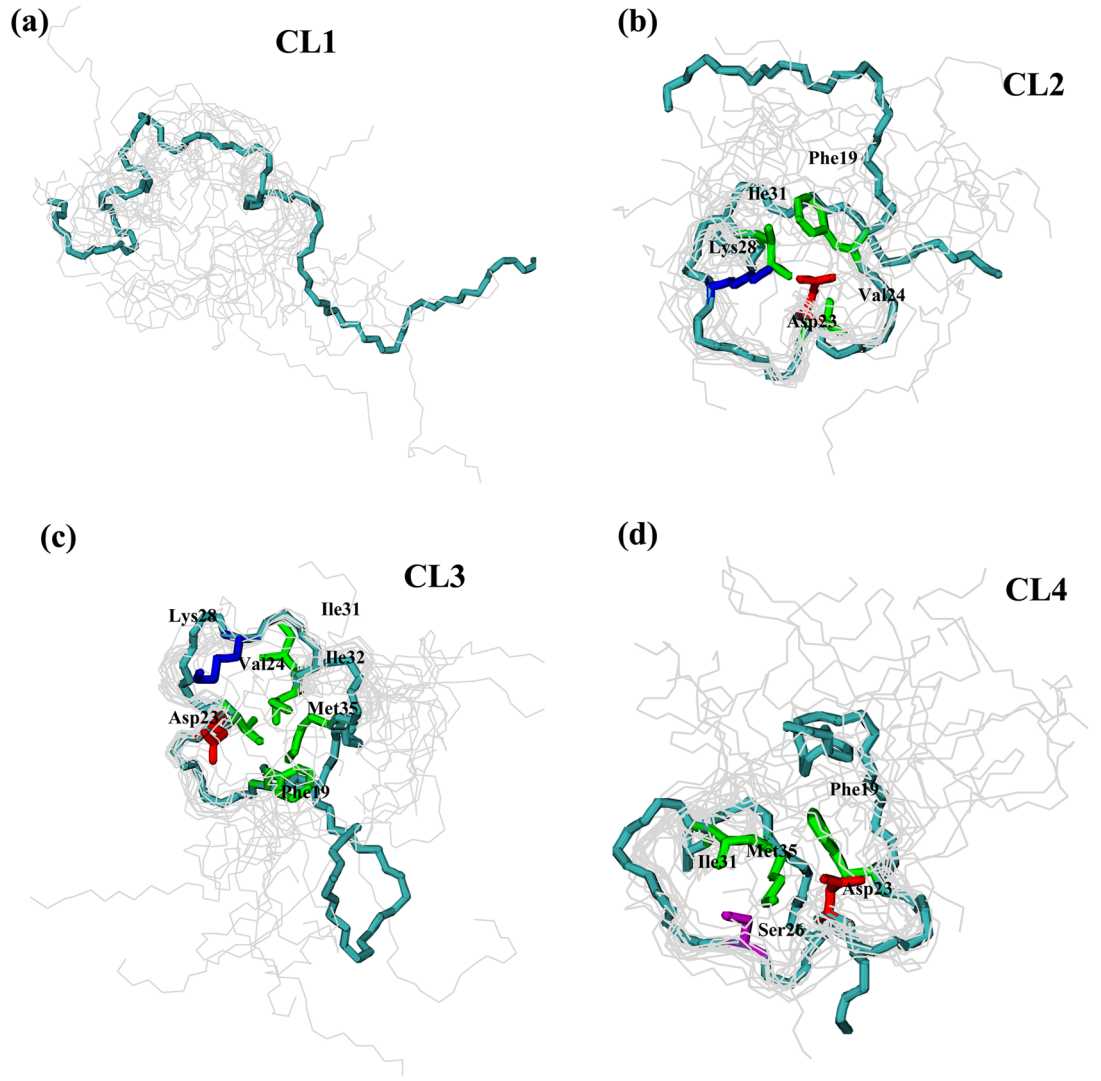

Figure 5. Superposition of Aβ structures from the conformational clusters is performed by minimizing the RMSD for the peptide region 19−35, which includes the structured regions R1 and R2. (a) Open cluster CL1 does not contain stable long-range contacts. (b) CL2 has four stable long-range interactions, most of which are formed by Ile31. Asp23-Lys28 salt bridge is formed. (c) The most structured is cluster CL3, which features six stable long-range contacts. Most of these interactions are formed by Val24 and Ile31. As in CL2 Asp23-Lys28 salt bridge is formed. (d) CL4 has four stable long-range contacts, most of which are formed by Ile31. Asp23-Lys28 salt bridge is broken. For each cluster a representative Aβ structure is drawn with the side chains involved in the stable long-range interactions. Hydrophobic side chains are colored in green. Asp23 and Lys28 side chains are in red and blue, respectively; polar side chains are in magenta. Backbones of other structures in a cluster are represented by thin gray lines. The conformational ensemble iscomputed for Aβ monomer in ibuprofen solution at 330 K.

Asp23-Lys28 salt bridge is $\Delta F_d^{\ddagger} = F_{TS} - F_{ON} = 2.9RT$. The barrier for forming the salt bridge has similar height ($\Delta F_a^{\ddagger} = F_{TS} - F_{OFF} = 3.0RT$). Figure 6 also demonstrates that the free energy barriers and gaps between the clusters CL1 and CL4 in the OFF state and between CL2 and CL3 in the ON state are insignificant ($\lesssim 0.3RT$).

DISCUSSION

Mechanism of Ibuprofen Binding. Using REMD sampling, we have analyzed the affinities, energetics, and free energy landscape of ibuprofen binding to Aβ monomer. Our findings suggest that the main factor governing ibuprofen binding to Aβ is hydrophobic effect (Figure 2b). All amino acids forming the ibuprofen binding site (Phe20, Val24, Ala30, Ile32, Leu34, Met35, Val36) are hydrophobic and located in the structured peptide regions R1 and R2 (Figure 3). Furthermore, the ligand−amino acid interactions $\langle C_l(i)\rangle$ strongly correlate with the decrease in the relative hydrophobic accessible surface area $\langle h\mathrm{ASA}(i)\rangle$ caused by binding (Figure 2b). To provide further evidence that hydrophobic interactions are mainly responsible for ibuprofen binding, we present in Figure S7 the changes in the relative polar accessible surface area $\langle p\mathrm{ASA}(i)\rangle$ caused by binding. We observe that in contrast to $\langle h\mathrm{ASA}(i)\rangle$ the change in $\langle p\mathrm{ASA}(i)\rangle$ does not correlate with $\langle C_l(i)\rangle$. (In fact, negative correlation factor of −0.25 suggests a weak anticorrelation between both quantities.) The importance of hydrophobic effect for ibuprofen binding is consistent with high hydrophobicity of ibuprofen molecule. In the unbound state the total accessible surface area (ASA) of ibuprofen is 418 Å^2, whereas the total hydrophobic ASA is 344 Å^2 or 82% of the total ASA. Our finding that ibuprofen binding site in Aβ is composed of hydrophobic amino acids is consistent with the recent computational study of several aromatic ligands binding to Aβ17−42 trimers.[18] Those simulations revealed that central

dx.doi.org/10.1021/jp306208n | J. Phys. Chem. B 2012, 116, 12922−12932

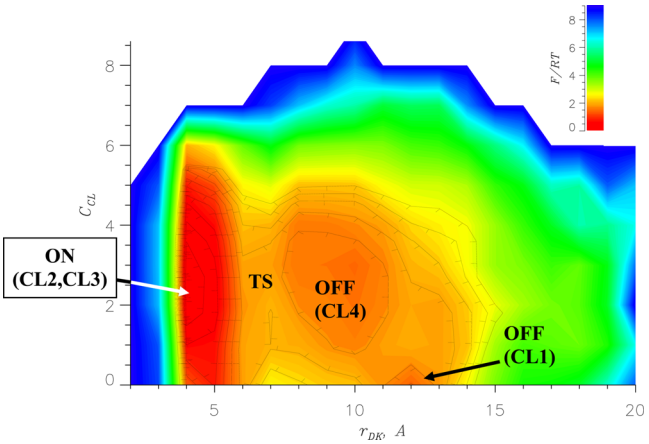

Figure 6. Free energy of Aβ peptide $F(r_{DK},C_{CL})$ is projected as a function of the distance between the side chains of Asp23 and Lys28, r_{DK}, and the number of intrapeptide contacts, C_{CL}, formed between the amino acids involved in stable interactions in CL1−CL4 clusters. The free energy landscape is computed at 330 K and color coded according to the scale. The states with formed (ON) and broken (OFF) Asp23-Lys28 salt bridge are marked. The approximate location of the transition state (TS) between ON and OFF is also indicated. Elevation contours are shown with 0.3RT interval. This plot suggests that Asp23-Lys28 salt bridge plays an important role in the conformational ensemble of Aβ monomer coincubated with ibuprofen.

hydrophobic cluster in Aβ17−42 serves as a primary binding location.

Interestingly, the contribution of hydrogen bonds to ibuprofen binding is minor. Indeed, the number of ligand−peptide hydrogen bonds $\langle N_{hb}\rangle$ (0.2) is more than 60 times smaller than the total number of ligand−peptide side chain contacts $\langle C_l\rangle$ (12.6). Such binding mode differs from the one observed recently for tricyclic ligands (9,10-anthraquinone and anthracene) binding to Aβ_{14-20} fibrils.[45] In contrast to ibuprofen, those ligands directly interfere with the formation of interstrand hydrogen bonds and reduce the accumulation of ordered aggregates. Participation of Phe20 in ibuprofen binding site raises the possibility of π-stacking interactions between the ligands and Phe. To explore this possibility, we have computed the distribution of the angle γ between the vectors normal to Phe20 and ibuprofen G1 aromatic rings. We distinguished two cases: the one in which ibuprofen is bound to Phe20 and the other in which ibuprofen is unbound. Two distributions of γ are nearly identical and consistent with random orientation of ibuprofen and Phe20 aromatic rings. Therefore, in the bound state ibuprofen G1 does not favor specific orientation with respect to Phe20, and the contribution of π-stacking interactions to binding appears to be limited. This result is consistent with the probabilities of binding ibuprofen groups to Phe20, which are 0.34 (G1), 0.45 (G2), and 0.13 (G3). These probabilities suggest that ibuprofen−Phe20 interactions are mostly driven by hydrophobic G2 isobutyl group, rather than aromatic G1. For other ligands π-stacking interactions can contribute to binding as has been recently demonstrated for curcumin binding to Aβ.[19]

At normal pH ibuprofen carboxylate group is deprotonated and negatively charged. It is therefore surprising that ibuprofen binding site does not include positively charged amino acids, Lys16 or Lys28. To rationalize this result, we compute the energy of nonbonded interactions formed by the Lys16 side chain. Consider the two states—(i) ibuprofen ligand(s) are bound to Lys16, but Lys16 does not form intrapeptide salt bridges (with Glu11, Glu22, or Asp23) and (ii) no ibuprofen ligands are bound to Lys16, but Lys16 forms intrapeptide salt bridge(s). The total energies of nonbonded interactions formed by Lys16 in these two states are −139 and −147 kcal/mol, respectively. Therefore, the formation of intrapeptide salt bridge (state ii) is energetically favorable because it reduces the Lys16 energy by 8 kcal/mol compared to state i. Similar reasoning explains relatively low binding affinity of Lys28. In summary, charged amino acids are unlikely to play an important role in ibuprofen binding to Aβ monomer due to competition from intrapeptide electrostatic interactions.

It is important to discuss the impact of N-terminal truncation on the binding of ibuprofen to Aβ. Our simulations suggest that the main factor in ibuprofen binding is hydrophobic effect and the binding sites are entirely composed of hydrophobic residues. Given highly polar characteristics of Aβ_{1-40} amino terminal it is unlikely that it serves as a primary binding location for ibuprofen comparable to those identified in Figure 2b. However, we cannot rule out the possibility that ibuprofen binds to Phe4 in Aβ_{1-40}, which may represent a secondary binding location.

According to our simulations the binding probability for ibuprofen is P_b = 0.44 at 300 K. If P_b is known, the dissociation equilibrium constant K_d can be computed as $K_d = [\mathrm{IBU}](1 - P_b)^2/P_b$, where [IBU] = 8 mM is the molar ibuprofen concentration in the simulations. Then, at 300 K, K_d = 6 mM, indicating that ibuprofen has low binding affinity with respect to Aβ peptides that may partially explain its modest efficiency as antiaggregation agent.[6−8]

The analysis of binding of two ibuprofen isomers, S and R, suggests that S has stronger binding affinity than R. Specifically, the probability of binding was found to be $P_b^S = 0.43 \pm 0.04$ for the S molecule compared to $P_b^R = 0.37 \pm 0.01$ for the R. This result is in qualitative agreement with the experimental measurements of the affinities of ibuprofen isomers binding to Aβ fibrils.[11] To investigate the origin of different isomer affinities, we have examined the energetics of the R and S binding. When bound ibuprofens self-aggregate, the energy of ligand−ligand interactions for the S isomer $\langle E_{ll}^S\rangle$ is 4.2 kcal/mol, whereas for the R $\langle E_{ll}^R\rangle$ = 2.3 kcal/mol. Therefore, S isomers repel other ligands stronger than Rs. Consequently, S isomers have fewer ligand neighbors in the bound clusters and are more exposed than Rs to the interactions with oppositely charged sodium ions in the solution. As a result, the energy of ligand−ion interactions for the S ($\langle E_{li}^S\rangle$ = −26.9 kcal/mol) is 3.7 kcal/mol lower than for the R ($\langle E_{li}^R\rangle$ = −23.2 kcal/mol). Note that other interaction energies for the bound S and R differ by less than 1 kcal/mol. This explanation is supported by the finding that no appreciable difference in the binding energetics is observed for the R and S isomers, which do not self-aggregate upon binding (i.e., for "stand-alone" bound ligands). In summary, the origin of tighter binding of the S isomer is apparently due to stronger repulsion between the ligands, resulting in more favorable interactions with ions. Therefore, the difference in binding affinities of the ibuprofen isomers may depend on the solution ionic strength. We would like to add a cautionary note that the findings presented above may depend on the specific ratio of R and S isomers. Because only one has been studied in this work, additional research specifically targeting different R and S ratios is needed to fully explore the energetics of R and S binding.

It is of interest to compare ibuprofen binding mechanisms proposed on the basis of explicit and implicit solvent simulations.[20,21] The latter predicts somewhat lower binding probability (0.22) at 330 K than the explicit solvent model (0.38). Furthermore, according to implicit solvent model the hydrophobic isobutyl G2 and polar G3 groups in ibuprofen form the strongest ligand−Aβ interactions. With respect to G2 this finding is consistent with the current study, in which we also found G2 to have the strongest binding affinity. Our implicit solvent simulations have also demonstrated that direct ligand−peptide as opposed to interligand interactions control naproxen binding to Aβ monomers.[24] A similar conclusion is reached in this study showing that ligand−peptide hydrophobic interactions govern the location of ibuprofen binding sites, whereas ligand−ligand interactions are unfavorable. However, explicit solvent model is at variance with implicit solvent simulations by predicting that the polar G3 group has small binding affinity. This difference is likely to be responsible for one other issue. According to implicit solvent model, the Aβ N-terminal (residues 10−23) forms about twice as many interactions with ibuprofen than the C-terminal (29−39). Explicit water simulations suggest that the binding site is distributed among the residues of the N- and C-terminals, with slight shift toward the latter (5.4 ligand−peptide contacts in the C-terminal vs 4.8 for the N-terminal). The third discrepancy between the two models is related to the propensity of bound ibuprofens to alter Aβ conformations, which is captured in explicit water simulations. This point is discussed below.

Conformational Ensemble of Aβ Peptide Coincubated with Ibuprofen. At 330 K, Aβ peptide coincubated with ibuprofen samples turn, helical, and random coil conformations with almost equal probabilities and forms two structured regions. The first region (R1, the residues 19−25) is dominated by turn and helix structure, whereas a stable helix emerges in the second region (R2, 29−35) (Figure 3). Other Aβ regions typically adopt a random coil structure. We have also shown that the most stable interactions include the contacts between the residues from the R1 and R2 (Phe19, Val24, and Ile31) and the salt bridge Asp23-Lys28. The analysis of conformational clusters and free energy landscapes provides further insight into Aβ ensemble (Figure 5), which consists of the structures, in which Asp23-Lys28 salt bridge is either formed (state ON) or disrupted (state OFF) (Figure 6). At 330 K, these two states have almost equal thermodynamic weights ($P_{OFF} \approx P_{ON} \approx \langle C(23,28)\rangle \approx 0.5$), and they are separated by a considerable free energy barrier of $\approx 3RT$. The structures composing the ON state populate the clusters CL2 and CL3, which differ with respect to the distribution of stable interactions between R1 and R2. In both clusters, which have similar occurrence probability, Ile31 and Val24 serve as interaction "hubs". The structures from the OFF state can be also grouped into two clusters, of which CL1 lacks stable long-range contacts, whereas the other (CL4) features stable hydrophobic interactions formed by the residue Ile31. Given a large free energy barrier separating the states ON and OFF and essentially barrierless paths connecting the clusters CL1 and CL4 in OFF and CL2 and CL3 in ON, we surmise that Aβ conformational ensemble is largely determined by the closure and rupture of the Asp23-Lys28 salt bridge.

Ibuprofen Changes Conformational Ensemble of Aβ Peptide. Important question pertains to the impact of ibuprofen binding on Aβ conformations. To investigate this issue, we performed control REMD simulations of Aβ peptide in ligand-free water system. Figure 7a shows the fractions of helical $\langle h(i)\rangle$, random coil $\langle rc(i)\rangle$, and turn $\langle t(i)\rangle$ structures

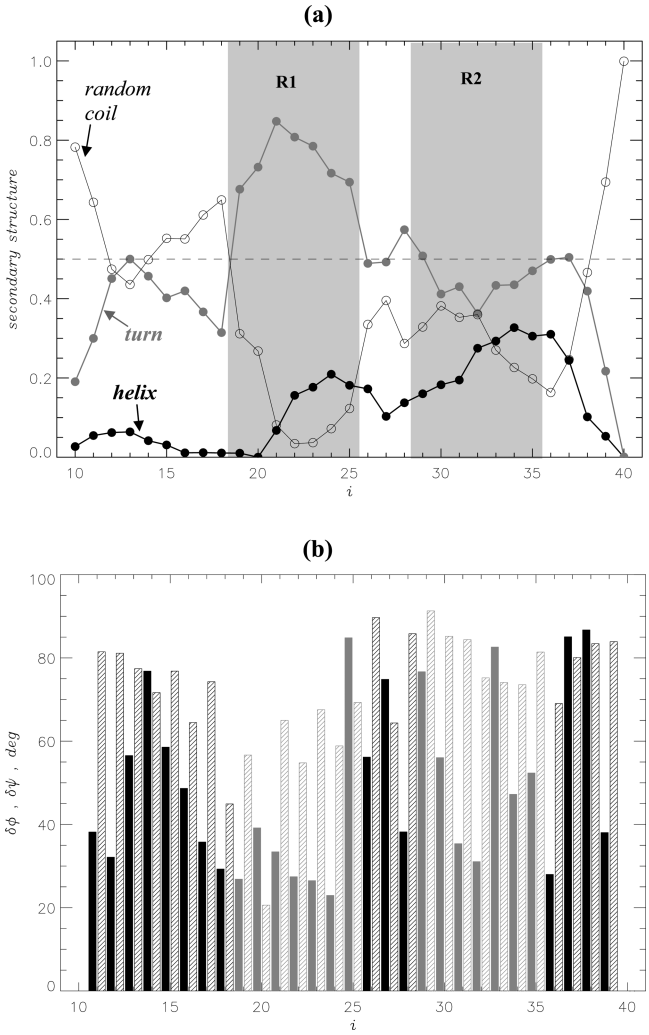

Figure 7. (a) Secondary structure in Aβ monomer in ligand-free water: fractions of helical $\langle h(i)\rangle$ (black filled circles), random coil $\langle rc(i)\rangle$ (open circles), and turn $\langle t(i)\rangle$ (gray filled circles) structure formed by residues i. Two regions R1 and R2 structured in Aβ monomer coincubated with ibuprofen are indicated. The plot is computed at 330 K using STRIDE. (b) Standard deviations, $\delta\phi(i)$ (filled bars) and $\delta\psi(i)$ (shaded bars), of the backbone dihedral angles ϕ and ψ for residues i in Aβ monomer in ligand-free water at 330 K. R1 and R2 regions structured in ibuprofen solution are shown in gray; the rest of the Aβ sequence is in black.

formed by individual residues i in water. Their distributions differ considerably from those observed in ibuprofen solution (Figure 3a). Specifically, the fraction of helix $\langle h\rangle$ decreases from 0.33 in ibuprofen solution to 0.13 for ligand-free environment. Simultaneously, the turn fraction increases from 0.35 to 0.48, whereas the random coil fraction undergoes minor changes (0.38 vs 0.32). The most dramatic restructuring occurs in the helix-rich region R2, where $\langle h(R2)\rangle$ is reduced from 0.74 to 0.25 in ligand-free water. The loss of helix structure is also observed around Val24. However, as in ibuprofen solution R1 region retains turn structure in water ($\langle t(R1)\rangle = 0.75$). Figure 7b offers further support for the disappearance of helix in ligand-free water by revealing the enhanced structural fluctuations in R2. For example, the average standard deviation

dx.doi.org/10.1021/jp306208n | J. Phys. Chem. B 2012, 116, 12922−12932

in ϕ and ψ in R2 increases from 38° to 68° that exceeds even the fluctuations in the unstructured Aβ regions in ibuprofen solution (61°). Finally, Figure 4b suggests that in contrast to ibuprofen solution the Asp23-Lys28 salt bridge is disrupted in water. Indeed, the probability of its formation is reduced to 0.17, and the average distance $\langle r_{DK} \rangle$ increases from 7.4 to 11.9 Å. Low probability of occurrence of Asp23-Lys28 salt bridge in water is consistent with the recent simulations of Aβ_{1-40} monomer.[46] Taken together, these findings indicate that ibuprofen binding changes Aβ structure by (i) inducing the formation of helix and (ii) stabilizing the Asp23-Lys28 salt bridge.

To explain the promotion of helix structure by ibuprofen, we have analyzed the ability of this ligand to form cross-bridges between amino acids i and $i + k$, where k is the cross-bridge length. (When a ligand forms a cross-bridge, it simultaneously interacts with the side chains of amino acids i and $i + k$.) Figure 2b displays the number of contacts $\langle C_{l,hcb}(i) \rangle$ associated with $k = 4$ cross-bridges, which are expected to stabilize α-helix structure. It follows from Figure 2b that in R2 $\langle C_{l,hcb}(R2) \rangle = 2.3$; i.e., helix-stabilizing ligand−Aβ contacts represents 51% of all ligand−Aβ contacts in this region ($\langle C_l(R2) \rangle = 4.6$). Elsewhere in A$\beta$ monomer the fraction of helix-stabilizing contacts is reduced to 0.32. The amino acids with the largest $\langle C_{l,hcb}(i) \rangle$ are Ala30, Ile32, Leu34, and Val36. According to our computations, more than 80% of helix-stabilizing contacts formed by these residues are related to only two specific cross-bridges, Ala30-Ibu-Leu34 and Ile32-Ibu-Val36. Elsewhere, the largest $\langle C_{l,hcb}(i) \rangle$ are observed for Phe20 and Val24 from R1, which are almost exclusively due to the formation of Phe20-Ibu-Val24 cross-bridge. Furthermore, our analysis suggests that more than half of all helix-stabilizing cross-bridges are formed by ibuprofen structural groups G1 and G2 or by G2 alone. Therefore, an appearance of helix structure in R2 and R1 (around Val24) is likely to be associated with ibuprofen binding, which "cross-links" amino acids sampling helical conformations.

The formation of helix structure in ibuprofen solution is consistent with recent experiments, which analyzed the impact of aggregation inhibitors on Aβ structure.[25] These studies have shown that inhibitor ligands generally increase Aβ helix content. The appearance of helix in response to ibuprofen binding may also be related to the observation that the sequence regions 15−24 and 29−35 in Aβ_{1-40} monomer adopt helical structure in membrane-like environment.[47,48] Interestingly, although the helix in the region 15−24 can be partially unraveled by the increase in pH above 6.0, the C-terminal helix-forming region, which corresponds to R2, remains stable.[47] These observations suggest that the C-terminal of Aβ harbors helical propensity, which can be revealed by membrane-like environment or ligand binding. It is more difficult to establish the reason promoting the formation of Asp23-Lys28 salt bridge. However, we suggest that near ibuprofen binding sites the environment for Aβ peptide is highly hydrophobic, and this factor reduces the local dielectric constant stabilizing electrostatic intrapeptide interactions. Finally, it should be noted that the formation of Asp23-Lys28 salt bridge affects local secondary structure. Upon its formation, the helix content in the sequence region Ala21-Ser26 increases from 0.22 to 0.58, whereas the turn fraction falls from 0.71 to 0.37. The random coil fraction remains unchanged, and the formation of this salt bridge has no impact on the secondary structure outside the Ala21-Ser26 region. Hence, Asp23-Lys28 interactions cause local conversion of turn conformations into helical structure.

Temperature Dependence of Ibuprofen Binding Mechanism. To probe temperature dependence of ibuprofen interactions with Aβ, we have considered binding of this ligand at 310 K. When recomputed at 310 K, Figure 2b reveals the same seven hydrophobic binding amino acids reported at 330 K. The number of ligand−Aβ contacts increases from 12.6 at 330 K to 13.8 at 310 K. The correlation between $\langle C_l(i) \rangle$ distributions computed at 310 and 330 K is very strong (correlation factor is 0.99). The peptide retains R1 and R2 structured regions and there are no significant changes in the secondary structure. For example, the helix fraction in R2 increases from 0.74 to 0.78. The overall fractions of helix, turn, and random coil are 0.35, 0.32, and 0.33, which are similar to those at 330 K. In summary, ibuprofen binding appears to weakly depend on temperature in the interval from 310 to 330 K.

Implications for Ibuprofen Antiaggregation Mechanism. Possible implications of our study for ibuprofen antiaggregation effect are as follows. First, we have shown that ibuprofen binding promotes helix structure in R2 and, to a lesser extent, in R1 Aβ regions. It is likely that the enhancement of helical structure by ibuprofen makes Aβ less prone for amyloid assembly. This possibility was recognized in the experimental study, which proposed that Aβ cytotoxicity can be reduced by designing the ligands which upon binding stabilize Aβ α-helix conformations.[49] A follow-up molecular dynamics study has demonstrated that the ligands, which upon binding cross-link the residues four positions apart, can at least delay the unfolding of helix in Aβ.[50] Second, our simulations suggest that ibuprofen binding promotes the formation of Asp23-Lys28 salt bridge. Its importance was demonstrated in the experimental study of Aβ_{1-40} lactam (D23/K28) mutant, in which Asp23 and Lys28 side chains were cross-linked.[51] It was found that this structural constraint speeds up Aβ aggregation 1000-fold compared to the wild-type. Therefore, ibuprofen binding may produce a complex effect on Aβ aggregation propensity by disfavoring amyloid formation by helix stabilization and simultaneously promoting aggregation by stabilizing Asp23-Lys28 salt bridge.

Ultimately, ibuprofen antiaggregation potential may depend on the third factor. We showed that ibuprofen binding to Aβ peptide is primarily governed by hydrophobic effect. Its binding site in Aβ is exclusively composed of hydrophobic amino acids from the central sequence region (Phe20 and Val24) and hydrophobic C-terminal (Ala30, Ile32, Leu34, Met35, and Val36). Experimental and computational studies have shown that these Aβ regions participate in aggregation interface.[52−57] Then, it is likely that ibuprofen antiaggregation effect involves interference with hydrophobic interactions between Aβ peptides. Taken together, we propose that the interplay of these three distinctive factors associated with ibuprofen binding limits the capacity of this ligand to act as inhibitor of Aβ aggregation. Future explicit solvent simulations directly probing ibuprofen interactions with Aβ oligomers will test our tentative antiaggregation mechanism.

CONCLUSIONS

In this study we used all-atom explicit water model and replica exchange molecular dynamics to investigate the interactions between Aβ monomer and nonsteroidal anti-inflammatory drug ibuprofen. Our results suggest that ibuprofen binding to Aβ is

largely governed by hydrophobic effect. Consequently, ibuprofen binding site in Aβ peptide is entirely composed of hydrophobic amino acids. Electrostatic interactions between negatively charged ibuprofen ligands and positively charged side chains make a weaker contribution to binding due to competition of ligand−peptide electrostatic interactions with intrapeptide salt bridges. In line with the experiments we predict that the S-isomer of ibuprofen binds with stronger affinity to Aβ than the R-isomer. The conformational ensemble of Aβ monomer in ibuprofen solution consists of two structured regions, 19−25 (R1) and 29−35 (R2), composed of turn/helix and helix structure, respectively. The clustering technique and free energy analysis suggest that Aβ conformational ensemble is mainly determined by the formation of Asp23-Lys28 salt bridge and the hydrophobic interactions between R1 and R2. Our control simulations of Aβ peptide in ligand-free water revealed that ibuprofen binding changes Aβ structure by promoting the formation of helix and Asp23-Lys28 salt bridge.

■ ASSOCIATED CONTENT

Ⓢ Supporting Information

Additional details concerning the model and methods used. This material is available free of charge via the Internet at http://pubs.acs.org.

■ AUTHOR INFORMATION

Corresponding Author

*E-mail: dklimov@gmu.edu.

Notes

The authors declare no competing financial interest.

■ ACKNOWLEDGMENTS

The authors thank Profs. A. Garcia and N. Sgourakis for providing experimental values of J coupling constants and Prof. Harvey for sending ibuprofen CHARMM parameters.

■ REFERENCES

(1) Hardy, J.; Selkoe, D. J. *Science* **2002**, *297*, 353−356.
(2) Haass, C.; Selkoe, D. J. *Nat. Rev. Mol. Cell Biol.* **2007**, *8*, 101−112.
(3) Dobson, C. M. *Nature* **2003**, *426*, 884−890.
(4) Shankar, G. M.; Li, S.; Mehta, T. H.; Garcia-Munoz, A.; Shepardson, N. E.; Smith, I.; Brett, F. M.; Farrell, M. A.; Rowan, M. J.; Lemere, C. A.; et al. *Nat. Med.* **2008**, *14*, 837−842.
(5) Xia, W. *Curr. Opin. Investig. Drugs* **2003**, *4*, 55−59.
(6) Akiyama, H.; Barger, S.; Barnum, S.; Bradt, B.; Bauer, J.; Cole, G. M.; Cooper, N. R.; Eikelenboom, P.; Emmerling, M.; Fiebich, B. L.; et al. *Neurobiol. Aging* **2000**, *21*, 383−421.
(7) Vlad, S. C.; Miller, D. R.; Kowall, N. R.; Felson, D. T. *Neurology* **2008**, *70*, 1672−1677.
(8) Imbimbo, B. P. *Expert Opin. Investig. Drugs* **2004**, *13*, 1469−1481.
(9) Heneka, M. T.; Sastre, M.; Dumitrescu-Ozimek, L.; Hanke, A.; Dewachter, I.; Kuiperi, C.; O'Banion, K.; Klockgether, T.; van Leuven, F.; Landreth, G. E. *Brain* **2005**, *128*, 1442−1453.
(10) McKeea, A. C.; Carrerasc, I.; Hossainc, L.; Ryua, H.; Kleine, W. L.; Oddof, S.; LaFerlaf, F. M.; Jenkins, B. G.; Kowalla, N. W.; Dedeoglua, A. *Brain Res.* **2008**, *1207*, 225−236.
(11) Agdeppa, E. D.; Kepe, V.; Petric, A.; Satyamurthy, N.; Liu, J.; Huang, S.-C.; Small, G. W.; Cole, G. M.; Barrio, J. R. *Neuroscience* **2003**, *117*, 723−730.
(12) Hirohata, M.; Ono, K.; Naiki, H.; Yamada, M. *Neuropharmacology* **2005**, *49*, 1088−1099.
(13) Ma, B.; Nussinov, R. *Curr. Opin. Struct. Biol.* **2006**, *10*, 445−452.
(14) Caflisch, A. *Curr. Opin. Chem. Biol.* **2006**, *10*, 437−444.
(15) Lemkul, J. A.; Bevan, D. R. *Biochemistry* **2010**, *49*, 3935−3946.
(16) Wu, C.; Bowers, M. T.; Shea, J. E. *Biophys. J.* **2011**, *100*, 1316−1324.
(17) Convertino, M.; Vitalis, A.; Caflisch, A. *J. Biol. Chem.* **2011**, *286*, 41578−41588.
(18) Chebaro, Y.; Jiang, P.; Zang, T.; Mu, Y.; Nguyen, P. H.; Mousseau, N.; Derreumaux, P. *J. Phys. Chem. B* **2012**, *116*, 8412−8422.
(19) Zhao, L. N.; Chiu, S. W.; Benoit, J.; Chew, L. Y.; Mu, Y. *J. Phys. Chem. B* **2012**, *116*, 7428−7435.
(20) Raman, E. P.; Takeda, T.; Klimov, D. K. *Biophys. J.* **2009**, *97*, 2070−2079.
(21) Chang, W. E.; Takeda, T.; Raman, E. P.; Klimov, D. K. *Biophys. J.* **2010**, *98*, 2662−2670.
(22) Takeda, T.; Chang, W. E.; Raman, E. P.; Klimov, D. K. *Proteins: Struct., Funct., Bioinform.* **2010**, *78*, 2859−2860.
(23) Takeda, T.; Kumar, R.; Raman, E. P.; Klimov, D. K. *J. Phys. Chem. B* **2010**, *114*, 15394−15402.
(24) Kim, S.; Chang, W.; Kumar, R.; Klimov, D. K. *Biophys. J.* **2011**, *100*, 2024−2032.
(25) Ryan, T. M.; Friedhuber, A.; Lind, M.; Howlett, G. J.; Masters, C.; Roberts, B. R. *J. Biol. Chem.* **2012**, *287*, 16947−16954.
(26) Buck, M.; Bouguet-Bonnet, S.; Pastor, R. W.; MacKerell, A. D. *Biophys. J.* **2006**, *90*, L36−L38.
(27) Bathelt, C. M.; Zurek, J.; Mulholland, A. J.; Harvey, J. N. *J. Am. Chem. Soc.* **2005**, *127*, 12900−12908.
(28) Bitan, G.; Vollers, S. S.; Teplow, D. B. *J. Biol. Chem.* **2003**, *278*, 34882−34889.
(29) Takeda, T.; Klimov, D. K. *J. Phys. Chem. B* **2009**, *113*, 6692−6702.
(30) Vitalis, A.; Caflisch, A. *J. Mol. Biol.* **2010**, *403*, 148−165.
(31) Ghidoni, R.; Albertini, V.; Squitti, R.; Paterlini, A.; Bruno, A.; Bernardini, S.; Cassetta, E.; Rossini, P. M.; Squitieri, F.; Benussi, L.; et al. *J. Alzheimer's Dis.* **2009**, *18*, 295−303.
(32) Thomas, T.; Nadackal, T. G.; Thomas, K. *NeuroReport* **2001**, *12*, 3263−3267.
(33) Bannwarth, B.; Lapicque, F.; Pehourcq, F.; Gillet, P.; Schaeverbeke, T.; Laborde, C.; Dehais, J.; Gaucher, A.; Netter, P. *Br. J. Clin. Pharmacol.* **1995**, *40*, 266−269.
(34) Mehta, P. D.; Parttila, T.; Mehta, S. P.; Sarsen, E. A.; Aisen, P. S.; Wisniewski, H. M. *Arch. Neurol.* **2000**, *57*, 100−105.
(35) Sugita, Y.; Okamoto, Y. *Chem. Phys. Lett.* **1999**, *114*, 141−151.
(36) Kale, L.; Skeel, R.; Bhandarkar, M.; Brunner, R.; Gursoy, A.; Krawetz, N.; Phillips, J.; Shinozaki, A.; Varadarajan, K.; Schulten, K. *J. Comput. Phys.* **1999**, *151*, 283−312.
(37) Sgourakis, N. G.; Yan, Y.; McCallum, S. A.; Wang, C.; Garcia, A. E. *J. Mol. Biol.* **2007**, *368*, 1448−1457.
(38) Kabsch, W.; Sander, C. *Biopolymers* **1983**, *22*, 2577−2637.
(39) Frishman, D.; Argos, P. *Proteins: Struct., Funct., Gen* **1995**, *23*, 566−579.
(40) Takeda, T.; Klimov, D. K. *Proteins: Struct., Funct., Bioinf.* **2009**, *77*, 1−13.
(41) Humphrey, W.; Dalke, A.; Schulten, K. *J. Mol. Graphics* **1996**, *14*, 33−38.
(42) Rose, G. D.; Geselowitz, A. R.; Lesser, G. J.; Lee, R. H.; Zehfus, M. H. *Science* **1985**, *229*, 834−838.
(43) Ferrenberg, A. M.; Swendsen, R. H. *Phys. Rev. Lett.* **1989**, *63*, 1195−1198.
(44) Petkova, A. T.; Yau, W.-M.; Tycko, R. *Biochemistry* **2006**, *45*, 498−512.
(45) Convertino, M.; Pellarin, R.; Catto, M.; Carotti, A.; Caflisch, A. *Protein Sci.* **2009**, *18*, 792−800.
(46) Tarus, B.; Straub, J. E.; Thirumalai, D. *J. Am. Chem. Soc.* **2006**, *128*, 16159−16168.
(47) Coles, M.; Bicknell, W.; Watson, A. A.; Fairlie, D. P.; Craik, D. J. *Biochemistry* **1998**, *37*, 11064−11077.
(48) Jarvet, J.; Danielsson, J.; Damberg, P.; Oleszczuk, M.; Graslund, A. *J. Biomol. NMR* **2007**, *39*, 63−72.
(49) Nerelius, C.; Sandegren, A.; Sargsyan, H.; Raunak, R.; Leijonmarck, H.; Chatterjee, U.; Fisahn, A.; Imarisio, S.; Lomas, D.

A.; Crowther, D. C.; et al. *Proc. Natl. Acad. Sci. U. S. A.* **2009**, *106*, 9191−9196.
(50) Ito, M.; Johansson, J.; Stromberg, R.; Nilsson, L. *PLoS One* **2012**, *7*, e30510.
(51) Scierretta, K. L.; Gordon, D. J.; Petkova, A. T.; Tycko, R.; Meredith, S. C. *Biochemistry* **2005**, *44*, 6003−6014.
(52) Fraser, P. E.; Nguyen, J. T.; Surewicz, W. K.; Kirschner, D. A. *Biophys. J.* **1991**, *60*, 1190−1201.
(53) Wurth, C.; Guimard, N. K.; Hecht, M. H. *J. Mol. Biol.* **2002**, *319*, 1279−1290.
(54) Urbanc, B.; Cruz, L.; Yun, S.; Buldyrev, S. V.; Bitan, G.; Teplow, D. B.; Stanley, H. E. *Proc. Natl. Acad. Sci. U. S. A.* **2004**, *101*, 17345−17350.
(55) Nandel, F. S.; Anand, P.; Hansmann, U. H. E. *J. Chem. Phys.* **2008**, *129*, 195102.
(56) Urbanc, B.; Betnel, M.; Cruz, L.; Bitan, G.; Teplow, D. B. *J. Am. Chem. Soc.* **2010**, *132*, 4266−4280.
(57) Melquiond, A.; Dong, X.; Mousseau, N.; Derreumaux, P. *Curr. Alzheimer Res.* **2008**, *5*, 244−250.